

# Polyethyleneimine Coating Enhances the Cellular Uptake of Mesoporous Silica Nanoparticles and Allows Safe Delivery of siRNA and DNA Constructs

Tian Xia,<sup>†,||</sup> Michael Kovochich,<sup>†,||</sup> Monty Liong,<sup>\*,||</sup> Huan Meng,<sup>†</sup> Sanaz Kabehie,<sup>‡</sup> Saji George,<sup>†</sup> Jeffrey I. Zink,<sup>\*,‡,⊥</sup> and Andre E. Nel<sup>†,§,⊥,\*</sup>

<sup>†</sup>Division of NanoMedicine, Department of Medicine, <sup>‡</sup>Department of Chemistry & Biochemistry, <sup>§</sup>The Southern California Particle Center, and <sup>⊥</sup>California NanoSystems Institute, University of California, Los Angeles, California 90095. <sup>||</sup>These authors contributed equally to this work.

**O**n the basis of properties such as large surface area and ordered porous channels that can be used to encapsulate molecules, mesoporous silica nanoparticles (MSNP) have emerged as an efficient drug delivery platform.<sup>1–5</sup> In addition to the well-developed surface chemistry, silica materials are known to be safe, biodegradable, and potentially biocompatible.<sup>6,7</sup> We and others have demonstrated that this drug transport system is suitable for the delivery of anticancer drugs, including camptothecin, paclitaxel, and doxorubicin.<sup>1,2,8</sup> The chemical stability of the particles contributes to their therapeutic utility by allowing the attachment of functional groups for imaging and targeting applications along with the placement of a series of nanovalves for on-demand drug release.<sup>2,9,10</sup>

In addition to being used for the delivery of chemical therapeutic agents, MSNP have the potential as hybrid organic–inorganic materials that can act as carriers for nucleic acids and therefore are potentially useful for the delivery of small interfering RNAs (siRNAs) and other forms of gene therapy.<sup>11–13</sup> As opposed to other gene delivery systems based on inorganic materials, the porous structure of MSNP allows both the binding of nucleotides on the surface as well as the encapsulation of small molecules within the particles. It is even possible to combine these modules to achieve dual delivery of drugs and nucleic acids.<sup>13</sup> To maximize the delivery of negatively charged nucleic acids to cells, the silica surface has

**ABSTRACT** Surface-functionalized mesoporous silica nanoparticles (MSNP) can be used as an efficient and safe carrier for bioactive molecules. In order to make the MSNP a more efficient delivery system, we modified the surface of the particles by a functional group that enhances cellular uptake and allows nucleic acid delivery in addition to traditional drug delivery. Noncovalent attachment of polyethyleneimine (PEI) polymers to the surface not only increases MSNP cellular uptake but also generates a cationic surface to which DNA and siRNA constructs could be attached. While efficient for intracellular delivery of these nucleic acids, the 25 kD PEI polymer unfortunately changes the safety profile of the MSNP that is otherwise very safe. By experimenting with several different polymer molecular weights, it was possible to retain high cellular uptake and transfection efficiency while reducing or even eliminating cationic MSNP cytotoxicity. The particles coated with the 10 kD PEI polymer were particularly efficient for transducing HEPA-1 cells with a siRNA construct that was capable of knocking down GFP expression. Similarly, transfection of a GFP plasmid induced effective expression of the fluorescent protein in >70% cells in the population. These outcomes were quantitatively assessed by confocal microscopy and flow cytometry. We also demonstrated that the enhanced cellular uptake of the nontoxic cationic MSNP enhances the delivery of the hydrophobic anticancer drug, paclitaxel, to pancreatic cancer cells. In summary, we demonstrate that, by a careful selection of PEI size, it is possible to construct cationic MSNP that are capable of nucleotide and enhanced drug delivery with minimal or no cytotoxicity. This novel use of a cationic MSNP extends its therapeutic use potential.

**KEYWORDS:** mesoporous silica nanoparticles (MSNP) · polyethyleneimine (PEI) · transfection · plasmid DNA · siRNA · drug delivery

to be converted into positive charge in order to bind DNA and siRNA. Some of the methods for introducing cationic charge on inorganic materials, which include silica, iron oxide, and gold, typically involve surface grafting with amine groups and coating with cationic polymers (*e.g.*, polyethyleneimine, polyamidoamine, and polylysine) through either covalent or electrostatic association.<sup>12,14–20</sup> The gene delivery capabilities of these surface-modified materials have been demonstrated and may prove useful as alternatives to traditional viral vectors.

\*Address correspondence to [anel@mednet.ucla.edu](mailto:anel@mednet.ucla.edu).

Received for review July 1, 2009 and accepted August 26, 2009.

Published online September 9, 2009. 10.1021/nn900918w CCC: \$40.75

© 2009 American Chemical Society

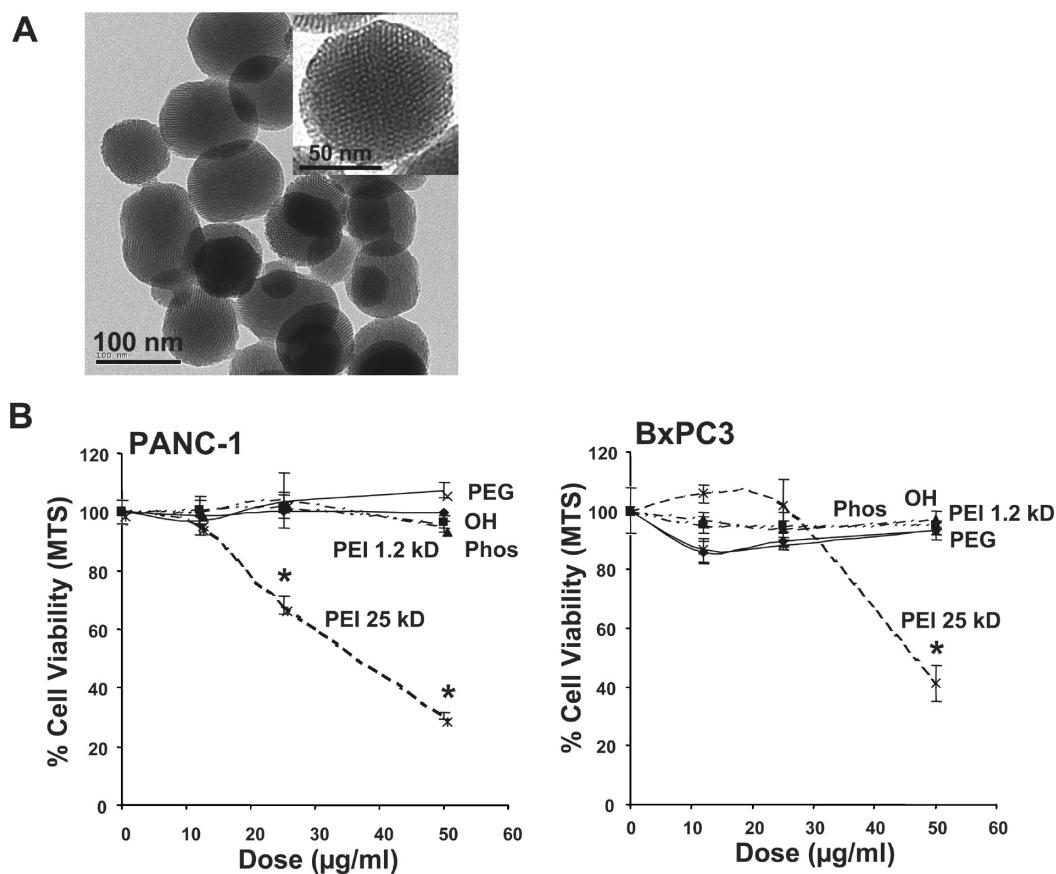


**Figure 1.** TEM of the MSNP and cell viability detection by the MTS assay. (A) TEM image shows the particle size and the ordered pore structure. (B) After addition of appropriately dispersed MSNP exhibiting a range of surface modifications to pancreatic cancer cell lines at doses ranging from 12.5 to 50  $\mu\text{g/mL}$  for 16 h, cells were incubated with the MTS reagent for 30 min and the absorbance was measured at 490 nm. All the MTS values were normalized according to the value of the control (no particle exposure); this was regarded as 100% cell viability. The  $\text{IC}_{50}$  values of MSNP-PEI-25 kD in PANC-1 and BxPC3 cells were 37 and 46  $\mu\text{g/mL}$ , respectively. The results were reproduced three times.

In this article, we studied the effects of polyethyleneimine (PEI) coating on the MSNP in terms of cellular uptake, cytotoxicity, and efficiency of nucleic acid delivery. PEIs are synthetic cationic polymers that compact DNA and siRNA into complexes that are effectively taken up in cells to make nucleic acid delivery and gene therapy possible.<sup>21–23</sup> Although the polymer itself is used as a delivery vehicle, PEI can also be attached to nanoparticle surfaces through covalent and electrostatic interactions to achieve the same goal.<sup>11,16,17,19,24</sup> Complexing the polymer with the nanoparticles has the potential advantage of facilitating DNA and siRNA delivery by a multifunctional platform that also allows imaging, targeting, and concurrent drug delivery. PEI was chosen as the polymer coating to enhance the particle uptake into cells and facilitate endosomal escape for the nucleotide delivery.<sup>25</sup> It is documented that, while low MW PEI is not cytotoxic, these polymers are ineffective at transfecting nucleotides in contrast to the high MW PEI. In this regard, it has been demonstrated that the size (MW), compactness, and chemical modification of PEI affect the efficacy and toxic-

ity of this polymer.<sup>26,27</sup> Therefore, we experimented with several PEI polymer sizes ranging from MW of 0.6 to 25 kD in order to balance the efficiency of nucleic acid delivery and cellular toxicity. PEI cytotoxicity occurs *via* a proton sponge effect, which involves proton sequestration by the polymer surface

**TABLE 1.** Size Distribution of MSNP in Aqueous Solutions<sup>a</sup>

	Size (nm)			$\zeta$ potential (mV)
	H <sub>2</sub> O	DMEM 10% serum	BEGM	H <sub>2</sub> O/DMEM + serum/BEGM + BSA
MSNP-OH	1966	408	1096	−10.5/−6.8/−7.2
MSNP-phosphate	1975	306	867	−8.9/−6.5/−5.8
MSNP-PEG	2675	405	1215	−10.4/−5.9/−4.5
MSNP-PEI 0.6 kD	1689	415	1243	+29.5/−7.8/−6.5
MSNP-PEI 1.2 kD	1684	452	1298	+38.7/−6.5/−7.1
MSNP-PEI 1.8 kD	1053	510	1087	+36.9/−5.4/−3.2
MSNP-PEI 10 kD	614	702	917	+34.1/−7.5/−6.9
MSNP-PEI 25 kD	1473	1043	1544	+30.8/−5.9/−4.0

<sup>a</sup>Particle size and  $\zeta$  potential in solution were measured by a ZetaSizer Nano (Malvern). DMEM = complete Dulbecco's Modified Eagle Media, which contains 10% fetal calf serum (FCS). BEGM = bronchial epithelial growth medium, which includes growth factors, cytokines, and supplements (no serum).

that leads to heightened proton pump activity inside the cell, osmotic swelling of the endocytic compartment, endosomal rupture, and ultimately cell death by a mitochondrial-mediated mechanism.<sup>28,29</sup> We demonstrate that the reduction of the polymer size is capable of scaling back the cytotoxic effect and that particles coated with polymers of 10 kD or less still maintain the feature of facilitated cellular uptake of cationic nanoparticles, most likely due to high avidity membrane binding and efficient membrane wrapping that allows these particles to enter cellular endocytic compartments. We show that the cellular uptake of PEI-coated MSNP, irrespective of polymer size, is considerably enhanced compared to unmodified MSNP (silanol surface) or particles coated with phosphonate or poly(ethylene glycol) groups. Finally, we demonstrate that PEI-coated particles bind plasmid DNA and siRNA with high affinity, enabling us to achieve efficient cellular delivery of these nucleic acids with non-toxic MSNP coated with 10 kD PEI.

## RESULTS

### Physicochemical Characterization

**of the NP.** MSNP were synthesized according to a modified procedure previously described.<sup>12,30</sup> The primary particle size is in the 100–130 nm range with a uniform pore size of  $\sim 2.5$  nm, as shown by TEM (Figure 1A). To conduct biological experimentation, particle size and  $\zeta$  potential were measured in water as well as tissue culture media.<sup>31</sup> For the purposes of this study, we used DMEM supplemented with 10% fetal calf serum (FCS) or BEGM as is or supplemented with 2 mg/mL BSA (Table 1). We observed that the addition of protein leads to improved particle dispersion by counteracting the colloidal forces that promote particle aggregation in salt containing media (Supporting Information Figure 1). While all of the non-PEI-coated particles exhibited a negative  $\zeta$  potential, PEI-coated particles showed a positive charge (Table 1). However, with the addition of FCS or BSA, all PEI-coated particles assumed negative  $\zeta$  potential.

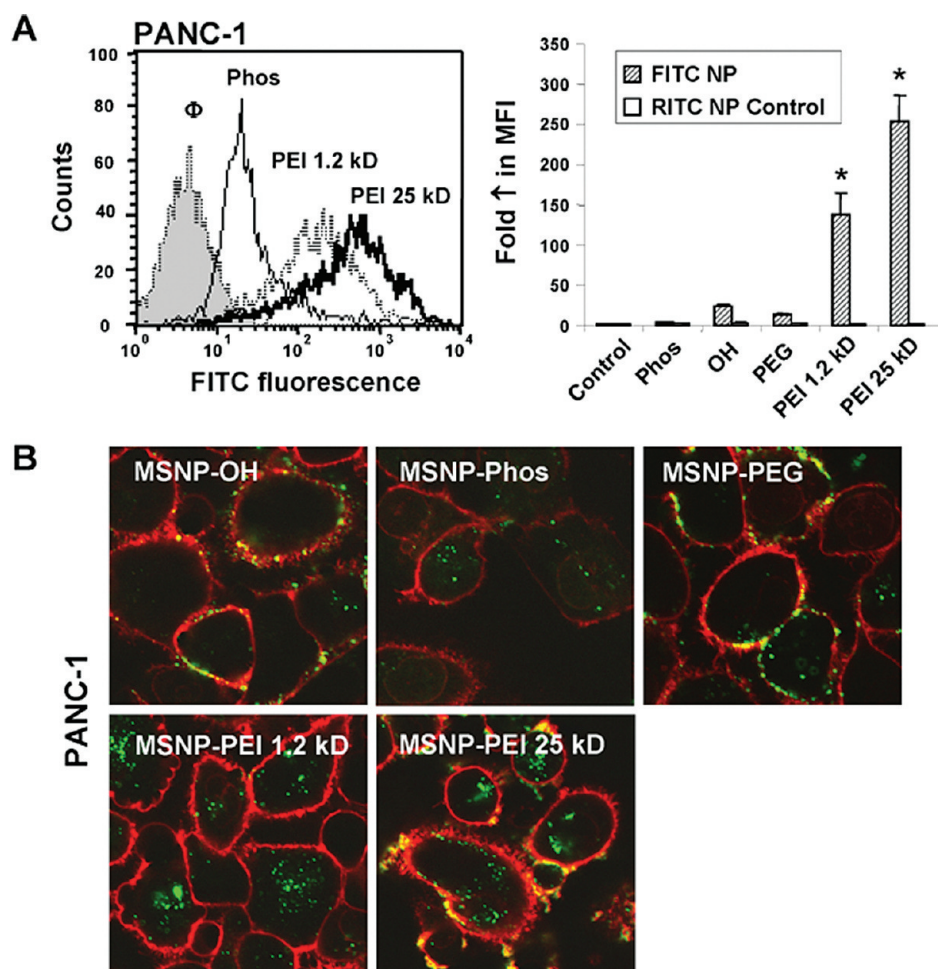


**Figure 2.** Cellular uptake of FITC-labeled MSNP in PANC-1 cells. MSNP were labeled with FITC as described in Materials and Methods. (A) Representative histogram showing the shift in fluorescence intensity in PANC-1 cells treated with 25  $\mu\text{g/mL}$  FITC-MSNP that contain different surface modifications (left panel). The fold increase in MFI after 3 h was calculated and used to generate the graph. RITC-labeled MSNP-Phos served as a control particle to show that coating with PEI leads to enhanced uptake in the same particle type in the same cell (right panel). (B) Confocal microscopy was used to study the cellular uptake of FITC-MSNP in PANC-1 cells. Cells were exposed to 25  $\mu\text{g/mL}$  FITC-labeled particles for 3 h. After cell membrane staining with 5  $\mu\text{g/mL}$  red-fluorescent wheat germ agglutinin (WGA), cells were visualized using a confocal 1P/FCS inverted microscope. Data are representative of three separate experiments;  $*p < 0.01$  compared with control.

### Differences in the Cytotoxic Potential of Anionic versus Cationic

**MSNP.** To screen for particle hazard, we used the MTS assay, which reflects dehydrogenase activity in healthy cells.<sup>29</sup> While most of the MSNP did not interfere in MTS activity in the PANC-1 and BxPC3 pancreatic cancer cell lines, particles coated with the 25 kD PEI polymer showed decreased cellular viability (Figure 1B). The particles coated with the 25 kD polymer also induced toxicity in macrophage (RAW 264.7) and bronchial epithelial (BEAS-2B) cell line staining (Supporting Information Figure 2). The toxicity was confirmed by propidium iodide (PI) staining, which showed that the rate of cell death was progressive over 15 h period (Supporting Information Figure 2). We also confirmed that, similar to our previous results with cationic polystyrene nanoparticles,<sup>29</sup> the toxicity of cationic MSNP involves an effect on mitochondria as determined by JC-1 fluorescence (Supporting Information Figure 2). JC-1 measures mito-



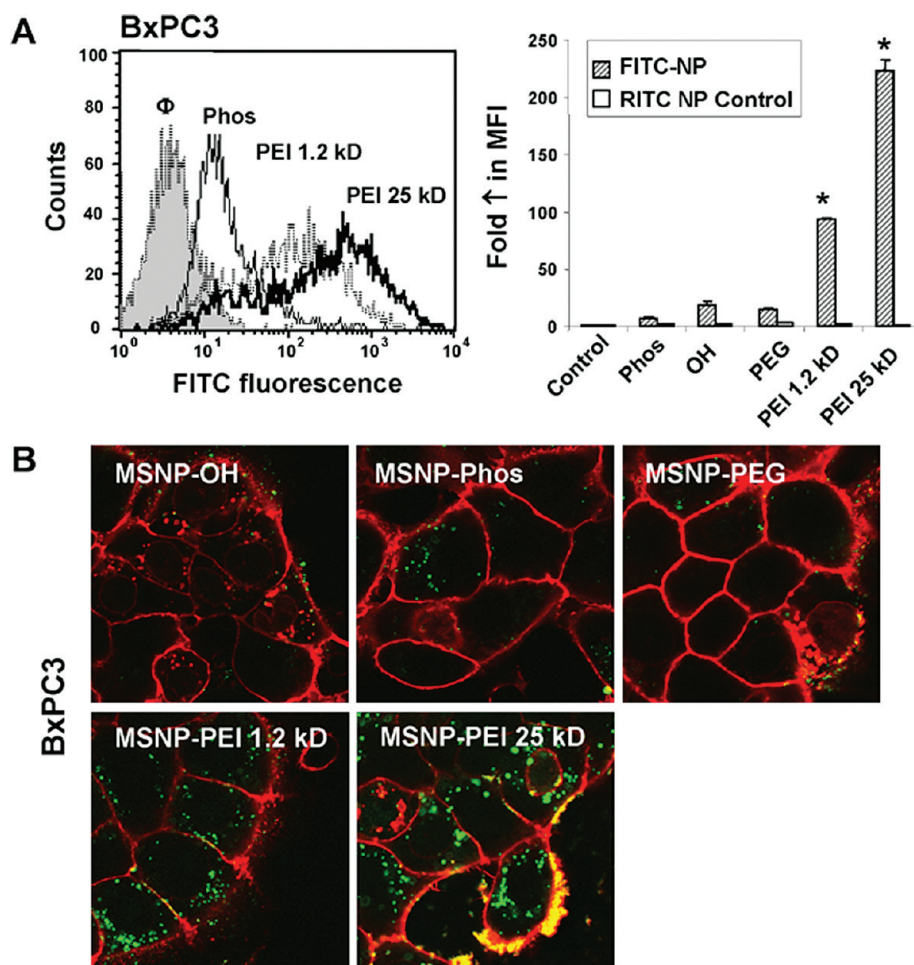


**Figure 3.** Cellular uptake of FITC-labeled MSNP in BxPC3 cells. BxPC3 cells were exposed to FITC-labeled MSNP, and flow cytometry and confocal microscopy were conducted as in Figure 2. Panels A and B represent similar observations.

chondrial membrane potential (MMP). In contrast, phosphonate-coated nanoparticles (MSNP-Phos) were nontoxic and did not perturb the mitochondrial function (Supporting Information Figure 2).

To confirm that PEI toxicity is due to cationic charge, succinic anhydride was used to convert the primary  $\text{NH}_2$  to  $\text{COOH}$  groups.<sup>29</sup> Supporting Information Figure 3A demonstrates that this conversion reduced the toxicity of MSNP-PEI-25 kD in a dose-dependent fashion. Depletion of the primary  $\text{NH}_2$  groups was confirmed by fluorescamine, which yields green fluorescence when it reacts with primary amines (Supporting Information Figure 2B). Thus, succinic anhydride reduced the mean fluorescence intensity (MFI) in a dose-dependent fashion. The stability of PEI attached to the MSNP surface was confirmed by coating FITC-labeled MSNP with rhodamine-B-labeled PEI. Confocal microscopy confirmed that both labels colocalize as shown by the composite yellow fluorescent spots in the cell (Supporting Information Figure 4).

**Differences in the Cellular Uptake of Anionic versus Cationic MSNP.** We have previously shown that the cellular toxicity of cationic polystyrene nanoparticles involves

a high rate of cellular uptake due to tight surface membrane binding, which facilitates particle wrapping and cellular uptake.<sup>28,29</sup> Cellular uptake of FITC-labeled MSNP was assessed by flow cytometry and confocal microscopy.<sup>29</sup> FITC-labeled MSNP were incubated with PANC-1, BxPC3, RAW 264.7, and BEAS-2B cells. This resulted in a clear shift in the MFI of the different cellular populations following treatment with particles coated with 1.2 and 25 kD PEI polymers as compared to the phosphonate-coated MSNP (Figures 2 and 3; Supporting Information Figure 5). When expressed as fold increase in the MFI compared to untreated cells, the relative abundance of MSNP-PEI-25 kD and MSNP-PEI-1.2 kD uptake was 2 orders of magnitude higher than the phosphonate or PEG-coated particles (Figures 2 and 3; Supporting Information Figure 5). In contrast, there was no difference in the uptake of RITC-labeled MSNP in the same cells treated with the FITC-labeled particles. This confirms that the cationic charge is responsible

for high cellular uptake. The flow data were corroborated by confocal studies that showed a significant increase in the number of PEI-coated particles in all cell types (Figures 2 and 3 and Supporting Information Figure 5). Please notice that a large fraction of the MSNP-PEI-25 kD particles localized at the cell membrane as demonstrated by the composite yellow fluorescence in pancreatic cancer cells stained with the red-fluorescent wheat germ agglutinin (Figures 2 and 3). It is possible that this membrane binding might contribute to the toxicity of these particles.

**Reducing PEI Polymer Length Maintains Effective Nucleic Acid Delivery but Eliminates Cellular Toxicity.** While PEI is quite effective for complexing and delivering nucleic acids, polymer-based delivery of DNA and siRNA often leads to cytotoxicity due to damage to the surface membrane, lysosomes, and mitochondria.<sup>21,26,29</sup> However, on the basis of the observation that decoration of MSNP with a 1.2 kD polymer resulted in a nontoxic particle, we explored the effect of a range of PEI polymers in terms of achieving cellular delivery versus reduction of toxicity. MSNP were coated

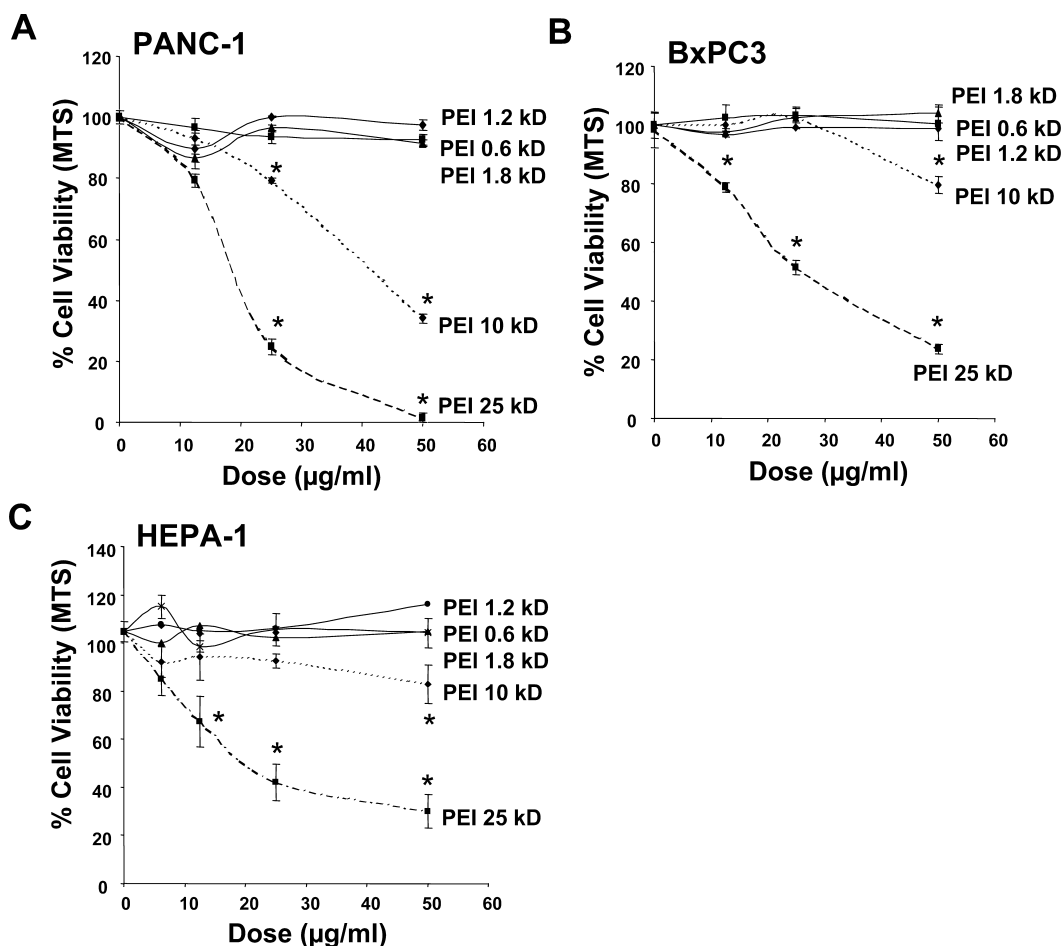


**Figure 4.** Cell viability detection by the MTS assay. After incubation with particles coated with polymers of MW 0.6–25 kD at doses of 6–100  $\mu\text{g}/\text{mL}$  for 16 h, PANC-1, BxPC3, and HEPA-1 cells were incubated with the MTS reagent for 30 min and the absorbance was measured at 490 nm. All the MTS values were normalized as described in Figure 1. The experiment was reproduced three times.

with 0.6, 1.2, 1.8, 10, and 25 kD polymers and their cytotoxic potential assessed in various cell types. This included the use of HEPA-1 cells for which there is a commercial variant expressing green fluorescent protein (GFP) for the purposes of assessing siRNA knockdown. No toxicity was seen with particles coated with 0.6, 1.2, and 1.8 kD PEI polymers (Figure 4 and Supporting Information Figure 6). While MSNP-PEI 10 kD exerted toxic effects at the highest dose (50  $\mu\text{g}/\text{mL}$ ) tested, MSNP-PEI 25 kD was responsible for the decline in MTS activity at doses  $\geq 12.5$   $\mu\text{g}/\text{mL}$  (Figure 4 and Supporting Information Figure 6). This demonstrates that it is possible to adjust MSNP toxicity according to the polymer length used and is the first demonstration that the choice of the PEI polymer length can be used to modify the toxicity of MSNP while still maintaining a useful function.

To assess the efficacy of different PEI-coated MSNP in terms of siRNA and plasmid DNA delivery, we first determined the nucleic acid binding capacity of the particles using a gel retardation assay. The data show high siRNA and plasmid DNA binding capacity that was

mostly independent of the PEI MW (Figure 5). All available DNA and siRNA molecules were bound to the cationic particle surface at particle-to-nucleic acid ratios of 10–100 (Figure 5B). Noteworthy, the high binding efficacy of MSNP was accompanied by protection of DNA to DNase I degradation (Figure 5C). By contrast, phosphonate-coated particles did not show effective DNA binding.

To test whether siRNA delivery to its GFP-expressing HEPA-1 cells could provide knockdown of the expression of this fluorescent protein, 100 ng of GFP-siRNA was complexed with MSNP-PEI and incubated with the cells for 48 h. Comparison of the MFI of transfected *versus* control cells showed that particles coated with 10 and 25 kD polymers were capable of knocking down GFP expression by 55 and 60%, respectively (Figure 6A). This was comparable to the transfection efficiency of commercially available transfection agent, Lipofectamine 2000. By contrast, scrambled siRNA delivery did not have a GFP knockdown effect (Figure 6A). Moreover, siRNA delivery by 0.6, 1.2, and 1.8 kD PEI-coated particles did not exert an effect on GFP expression. GFP knock-

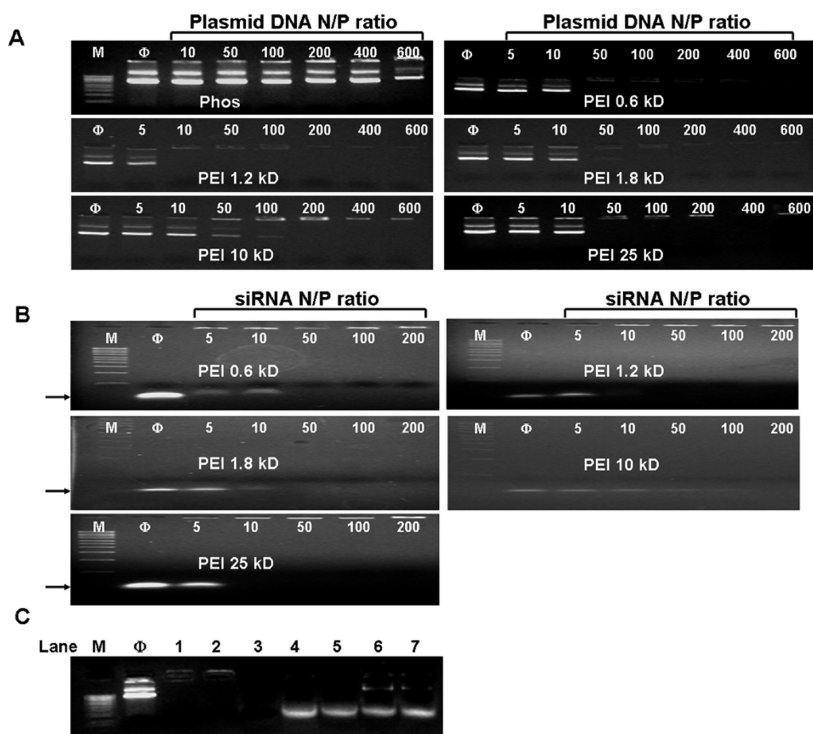


**Figure 5.** Gel retardation and DNase I protection assays. Agarose gel electrophoresis of PEI-MSNPs/plasmid DNA (pEGFP) (A) and PEI-MSNPs/siRNA (B) complexes at various nano-particle to nucleic acid (N/P) ratios. Anionic phosphonate-coated MSNP was used as a control. M = MW marker. (C) DNase I protection assay. M: DNA marker.  $\Phi$ : naked plasmid DNA (pEGFP), as negative control. Lane 1, pDNA/PEI 1.2 kD complex. Lane 2, pDNA/PEI 25 kD complex. Lane 3, naked pDNA treated with DNase I, positive control. Lane 4, pDNA/PEI 1.2 kD complex treated with DNase I before pDNA was released by 1% SDS. Lane 5, pDNA/PEI 25 kD complex treated with DNase I before pDNA was released by 1% SDS. Lane 6, pDNA/PEI 1.2 kD complex treated with 1% SDS. Lane 7, pDNA/PEI 25 kD complex treated with 1% SDS.

down was confirmed by confocal microscopy (Figure 6B) and immunoblotting for GFP protein expression (Supporting Information Figure 7). Please notice that, although the toxicity of the 25 kD polymer may contribute to decreased GFP expression, the 10 kD polymers are not toxic at this dose (Figure 4). Scrambled siRNA delivery had no effect on GFP expression (Figure 6B). Confocal studies using Texas Red-labeled siRNA were performed to track the intracellular fate of the particles (Figure 6B). This confirmed that the particles coated with longer polymers were taken up in larger numbers than the shorter range polymers in HEPA-1 cells (Figure 6B and Supporting Information Figure 7B).

In the next set of experiments, we assessed the efficacy of DNA delivery by transfecting a GFP plasmid into HEPA-1 cells. While plasmid delivery by the 10 and 25 kD PEI-coated particles resulted in abundant cellular fluorescence, only faint fluorescence was observed when the carrier particle was coated with a shorter length polymer (Figure 7). The transfection efficiency with the longer length polymers compares favorably to the results with Lipofectamine 2000. Moreover, while this commercial agent only transduced a fraction of the cells in the population, MSNP-PEI 10 kD transfected

>70% cells in the population (Figure 7B).

This was confirmed by the magnitude of the MFI increase with the particles versus Lipofectamine 2000 (Figure 7A). Although also efficient for DNA delivery, MSNP-PEI 25 kD did result in toxicity as explained previously. This may not constitute a problem when stable transfections are being performed because one selects for viable and proliferating cells containing the expressed gene.

#### Cationic MSNP is Effective for Delivering Paclitaxel to Pancreatic Cancer Cells.

We have recently demonstrated that MSNP are capable of delivering water-insoluble drugs to cancer cells.<sup>2</sup> In light of the high cellular uptake of PEI-coated particles, it was logical to ask whether, in the traditional use of the MSNP, the polymer attachment still allows effective delivery of the hydrophobic cancer drug, paclitaxel, to PANC-1 and BxPC3 cells. Paclitaxel was loaded into MSNP-PEI 1.2 kD and 25 kD in DMSO, followed by washing in aqueous buffer to entrap the hydrophobic drug in the particle pores. Release of the drug from the pores using methanol confirmed that equal amounts of paclitaxel were loaded into MSNP irrespective of the polymer MW (Supporting Information Figure 8). Subsequent assessment of the impact of paclitaxel on the viability of PANC-1 and BxPC3 cells showed the efficacy of PEI-coated MSNP in drug delivery (Figure 8). Thus, paclitaxel delivery by

MSNP-PEI 1.2 kD induced a rate of cytotoxicity that is superior to the drug delivery by an aqueous suspension of paclitaxel and as efficient as the drug suspended in DMSO (Figure 8). While MSNP-PEI 25 kD showed intrinsic particle-related toxicity at doses >25  $\mu\text{g}/\text{mL}$ , the effect was comparable to MSNP-PEI 1.2 kD (Figure 8). These data demonstrate that the enhanced cellular uptake of nontoxic cationic MSNP is capable of enhancing the delivery of hydrophobic cancer drugs. This is also a novel demonstration for the delivery function of MSNP.

**PEI-Coated MSNP Are Devoid of Toxicity *In Vivo*.** In order to achieve therapeutic delivery of nucleic acids and drugs, it is required that cationic particles are well-tolerated and without any evidence of toxicity *in vivo*. Hence, it was necessary for us to demonstrate that PEI-coated MSNP can be safely administered to animals, and we chose intravenous injection of 25 kD PEI-coated particles to perform this analysis. MSNP-phosphonate and saline-only injections were used as controls. Particles were injected *via* the tail vein at doses of 40 mg/kg once a week for 2 weeks. In order to keep the particles appropriately dispersed, it was necessary to stabilize them against aggregating effects of the saline carrier. Saline alone yielded par-



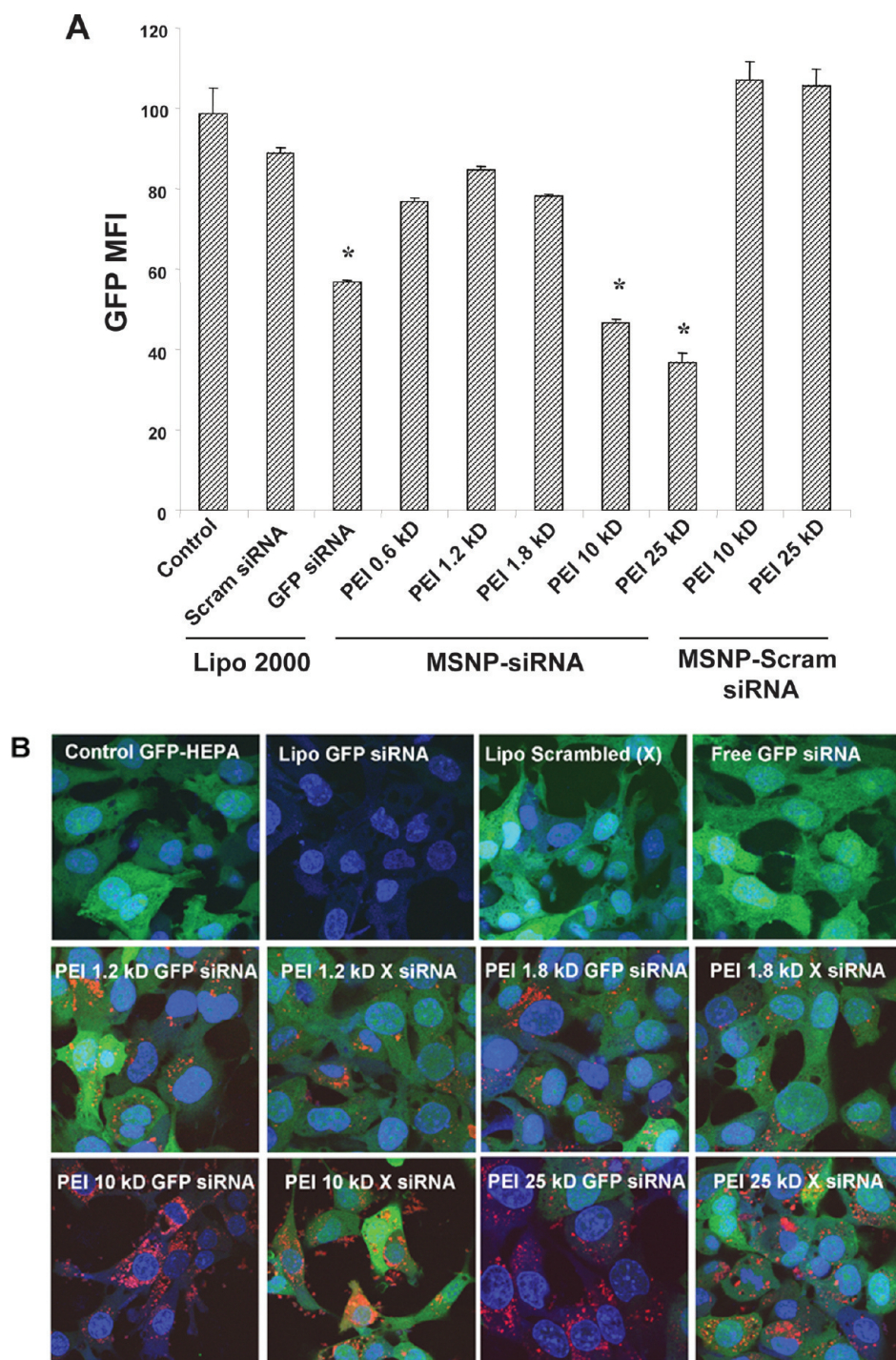


**Figure 6.** GFP knockdown by siRNA in stable transfected GFP-HEPA cells. HEPA-1 cells with stable GFP expression were used for siRNA knockdown assays. MSNP coated with different size PEI polymers were used to transfect GFP-specific or scrambled siRNA and the results compared with Lipofectamine 2000 as transfection agent. (A) GFP knockdown was assessed by flow cytometry in which GFP MFI was normalized to the value of control untransduced cells (100%). (B) Confocal pictures were taken showing GFP knockdown in GFP-HEPA cells. TEX 615-labeled siRNA was used to show the cellular localization of the nucleic acid bound particles (red dots). X, scrambled siRNA. The experiment was reproduced three times.

ticles sizes of 984 and 842 nm, respectively, for MSNP-phosphonate and MSNP-PEI 25 kD. Particle dispersion was improved by adding 2% mouse serum, which reduced the particle sizes to 249 and 278 nm, respectively, in saline. Animals were sacrificed 2 weeks after the first injection, and blood and major organs such as liver, kidney, spleen, lung, heart,

and brain were removed for study. Biochemical analysis of the serum did not show any significant changes in liver function, kidney function, cholesterol and triglycerides, glucose, CO<sub>2</sub> content, and electrolytes of PEI versus phosphonate particles or the saline control (Table 2). Moreover, histological examination of the major organs did not show any

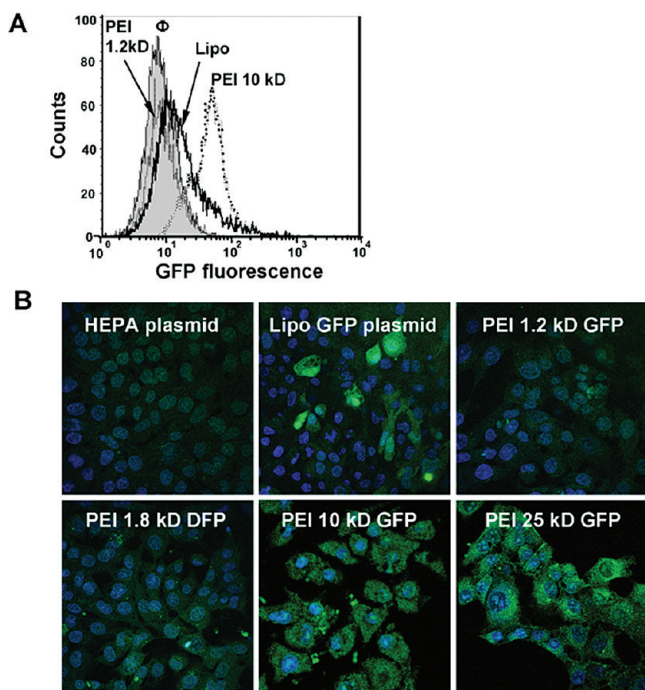


**Figure 7.** GFP plasmid DNA transfection into HEPA-1 cells. HEPA-1 cells were used for GFP plasmid DNA transfection. MSNP coated with different size PEI polymers were used to transfect GFP plasmid DNA, and the results were compared with Lipofectamine 2000 as transfection agent. (A) Representative histogram showing the shift in green fluorescence intensity in HEPA-1 cells after transfection with Lipofectamine 2000 or MSNP-PEI 10 kD. (B) Confocal pictures showing GFP expression in transfected HEPA-1 cells. This demonstrates differences in the transfection efficiency as judged by fluorescent intensity and proportion of cells in the population showing GFP expression. The experiment was reproduced three times.

gross pathology; representative liver, spleen, and kidney sections are shown in Supporting Information Figure 9. In summary, these data confirm the safety of phosphonate MSNP and demonstrate that particles coated with 25 kD PEI, which is responsible for considerable *in vitro* cytotoxicity, is also well-tolerated *in vivo*. This demonstrates that PEI-coated in MSNP could in principle be safely implemented for *in vivo* drug and siRNA delivery. However, for this to become a therapeutically useful option, additional experimentation is required to show that the circulatory half-life and pharmacokinetics of MSNP delivery system that can achieve effective drug and nucleic acid delivery.

## DISCUSSION

In this paper, we demonstrate that surface coating with PEI yields cationic MSNP with therapeutically useful nucleic acid delivery properties that include high binding avidity of DNA and siRNA as well as a high rate of cellular uptake. We show that siRNA complexed to the MSNP-PEI surface is quite effective to achieve GFP knockdown in transduced HEPA-1 cells, while plasmid DNA delivery is comparable to a commercially available transfection agent. We further demonstrate that the facilitated cellular uptake of cationic particles enhances

the ability of MSNP to deliver the hydrophobic chemotherapeutic agent, paclitaxel, to pancreatic cancer cells. A potential downside of cationic functionalization for drug or nucleic delivery is the possibility of cytotoxicity, best demonstrated by the use of MSNP-PEI 25 kD. However, we demonstrate that this toxicity could be reduced or eliminated by attaching shorter length polymers that retain nucleic acid and drug delivery capabilities. Moreover, injection of MSNP coated with PEI 25 kD did not lead to obvious toxicity *in vivo*. Thus, we demonstrate that the therapeutic use of the MSNP platform can be extended to delivery of DNA and siRNA constructs. From the perspective of MSNP as a therapeutic platform, these are novel and encouraging findings.

RNA interference describes natural processes that lead to gene silencing by siRNA.<sup>32</sup> siRNA has been widely used as an experimental tool that is now also becoming the focus of the pharmaceutical industry.<sup>33</sup> Currently, there are a number of clinical trials underway that include the use of siRNAs to treat various disease processes.<sup>34,35</sup> As for most molecular therapies, *in vivo* delivery is a major hurdle in successful implementation and has sparked a number of strategies to increase siRNA circulatory half-life, facilitate transduction across biological membranes, and achieve cell-specific delivery.<sup>34,35</sup> We propose that packaging of siRNA on the surface of cationic MSNP is capable of meeting each of these objectives. First, the MSNP surface can be functionalized to enhance siRNA binding through the attachment of PEI polymers, which in their own right have been used as effective siRNA compacting and transducing agents. The tight complexing between PEI and nucleic acids on the particle surface protects these molecules from enzymatic degradation as we demonstrated for DNA. Furthermore, the positive charge of PEI-coated nanoparticles leads to strong electrostatic interaction with the negatively charged cell surface membrane, leading to facilitated particle wrapping and cellular uptake. This is in agreement with the recent demonstration that PEI-coated nanoparticles are taken up into cells at high efficiency.<sup>10,25</sup> However, the latter study did not look at nucleic acid delivery but did show that the attachment of a ligand such as folic acid further enhances uptake in cancer cells.<sup>2,10</sup> While PEI can be used in various ways to make siRNA delivery complexes, coating it onto the surface of MSNP is particularly advantageous because this therapeutic platform acts as a carrier with large surface area, is inexpensive and simple to synthesize, can be decorated with functional groups and fluorescent tags, and can be used for magnetic resonance imaging through the inclusion of superparamagnetic iron oxide nanocrystals.<sup>2</sup> Not only have we shown PEI coating can enhance siRNA delivery, but the particles also are capable of paclitaxel



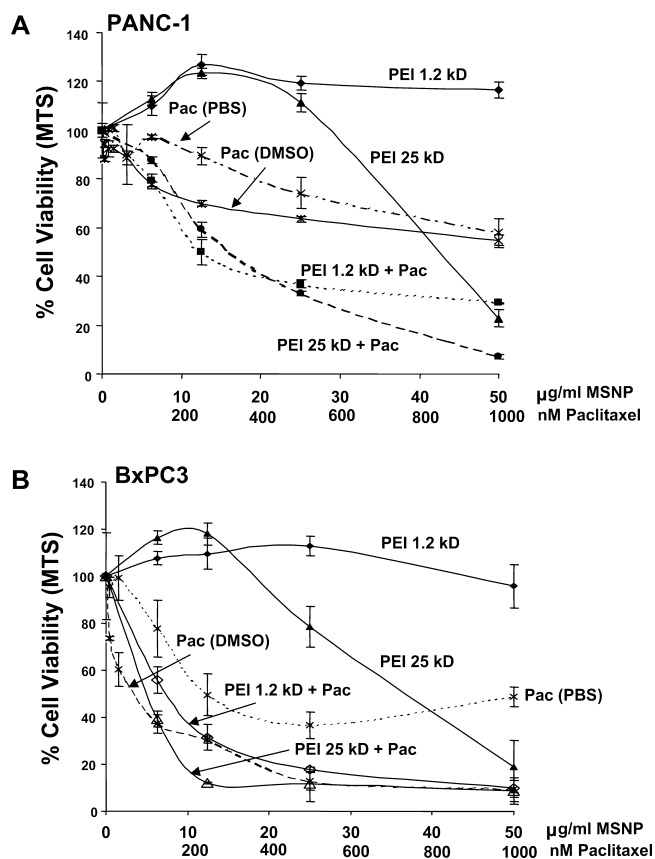


**Figure 8.** Drug delivery to PANC-1 and BxPC3 cells using PEI-MSNP. MTS assay was conducted for the paclitaxel-loaded MSNP delivered to these cells at doses of 3–50  $\mu\text{g}/\text{mL}$  over a 48 h period in (A) PANC-1 and (B) BxPC3 cells. The controls were cells treated with particles only and cells treated with paclitaxel suspended in culture medium with and without the addition of DMSO carrier. The experiment was reproduced two times.

delivery, which constitutes a significant therapeutic advance for MSNP. One can envisage using siRNA and drug delivery simultaneously, for example, delivery of siRNA that knocks down the expression of the P-glycoprotein (Pgp) drug exporter at the same time as delivering a chemotherapeutic agent that is exported by Pgp.<sup>36</sup> This could be an effective strategy for the treatment of cancers that have developed a drug resistance based on the activity of this exporter.

Several advantages of MSNP-PEI for the delivery of siRNA also hold true for plasmid DNA transduction. In fact, a number of modifications of the PEI polymer, including various polymer sizes, degrees of branching, thiol cross-linking, and covalent attachment, have been used as gene transfer agents since the 1990s and are enjoying increasing popularity because of the high transfection efficiency of plasmid DNA and siRNA into cells and live animals.<sup>21–23,37</sup> The advantage of using PEI for gene transfer lies in the simplicity with which the polymer can be mixed with DNA/siRNA without involving covalent attachment. Moreover, PEI protects the nucleic acids from degradation by nucleases. In all of

these therapeutic applications, however, one has to keep in mind that the high MW polymer could cause toxicity.<sup>26</sup> In a novel undertaking, we now show that it is possible to modify the potential basis for toxicity while maintaining effective nucleic acid delivery by using intermediate length polymers. We show how these intermediate length polymers lead to effective cellular uptake and siRNA/plasmid DNA delivery. Moreover, our approach leads to transfection of >70% cells in the population, which is clearly advantageous from the perspective of gene therapy.

Other than mediating its effect through high cellular uptake, the efficient gene transduction ability of PEI proceeds *via* the proton sponge effect, implying that the primary amines buffer the protons being pumped into the lysosomal compartment by the v-ATPase (proton pump).<sup>21,29,38</sup> This results in heightened pump activity, leading to the accumulation of a  $\text{Cl}^-$  and a water molecule for each proton that is retained; ultimately, this leads to osmotic rupture of the endosome.<sup>39</sup> While effective for delivering the nucleic acid cargo to the cytosol, the effect of PEI or cationic particles on the proton pump is a major contributory factor in cationic cytotoxicity.<sup>29</sup> Cationic nanoparticle toxicity can lead to clinically significant adverse health effects.<sup>40–42</sup> Methods to reduce cationic toxicity but

leaving cargo delivery intact are highly desired.<sup>43</sup> Experimental examples of how PEI toxicity has been reduced include neutralizing the cationic charge by anhydride, differential ketalization, altering PEI cross-linking through adjustment of disulfide content, and using shorter polymers.<sup>29,44–47</sup> We demonstrate that the latter principal can also be applied to PEI-coated MSNP, where we have been able to reduce or eliminate cytotoxicity while maintaining efficient nucleic acid delivery. Thus, by attaching a 10 kD polymer, we were able to demonstrate that it was possible at particle doses <50  $\mu\text{g}/\text{mL}$  to obtain highly efficient transduction without any cell death. Our data also indicate that the PEI-coated MSNP can be intravenously injected into mice without causing acute toxicity. It appears, therefore, that cationic toxicity can be controlled to achieve a therapeutically useful outcome. While the gene transduction efficiency is significantly reduced with lower MW (0.6–1.8 kD) polymers, the facilitated MSNP uptake is good enough to achieve efficient paclitaxel delivery (Figure 8).

While our study is mostly limited to demonstrating successful transduction across biological mem-

TABLE 2. Serum Biochemistry (avg  $\pm$  SD,  $n = 6$ )<sup>a</sup>

	control (saline)	MSNP-Phos	MSNP-PEI 25 kD
CHOL (mg/dL)	162.5 $\pm$ 8.5	153.8 $\pm$ 15.4	144.4 $\pm$ 6.8
CK (U/L)	3000.3 $\pm$ 2285.3	2690.5 $\pm$ 1129.3	3280.9 $\pm$ 1512.7
ALT (U/L)	59.5 $\pm$ 6.4	55.7 $\pm$ 8.4	46.1 $\pm$ 22.6
AST (U/L)	184.2 $\pm$ 70.2	182.2 $\pm$ 21.1	217.2 $\pm$ 65.6
ALP (U/L)	105.2 $\pm$ 8.6	102.1 $\pm$ 17.5	88.6 $\pm$ 48.9
TBILI (mg/dL)	0.7 $\pm$ 0.1	0.9 $\pm$ 0.3	0.6 $\pm$ 0.1
TPROT (mg/dL)	6.2 $\pm$ 0.2	6.0 $\pm$ 0.4	5.9 $\pm$ 0.3
GLU (mg/dL)	140.8 $\pm$ 16.5	141.2 $\pm$ 29.2	140.8 $\pm$ 34.6
PHOS (mg/dL)	8.4 $\pm$ 0.7	7.4 $\pm$ 1.0	8.3 $\pm$ 0.6
CA (mg/dL)	8.9 $\pm$ 1.7	9.2 $\pm$ 0.4	9.4 $\pm$ 0.2
CO <sub>2</sub> _LC (mEq/L)	10.1 $\pm$ 2.2	13.3 $\pm$ 3.8	11.3 $\pm$ 1.1
BUN (mg/dL)	20.8 $\pm$ 2.1	22.3 $\pm$ 9.3	22.6 $\pm$ 2.6
CREAT (mg/dL)	0.3 $\pm$ 0.0	0.3 $\pm$ 0.1	0.3 $\pm$ 0.0
D-BILI (mg/dL)	0.9 $\pm$ 0.2	1.0 $\pm$ 0.5	0.7 $\pm$ 0.2
ALB (g/dL)	3.3 $\pm$ 0.1	3.2 $\pm$ 0.2	3.2 $\pm$ 0.2
AGR (N/A)	1.2 $\pm$ 0.1	1.2 $\pm$ 0.1	1.1 $\pm$ 0.1
B-CREA (mg/dL)	75.3 $\pm$ 16.2	79.2 $\pm$ 30.0	82.0 $\pm$ 12.4
AMYL (U/L)	1252.2 $\pm$ 215.1	1266.0 $\pm$ 189.5	1139.4 $\pm$ 122.0
LDH (U/L)	681.5 $\pm$ 152.8	638.8 $\pm$ 133.3	611.0 $\pm$ 141.6
Mg (mg/dL)	2.0 $\pm$ 0.5	2.2 $\pm$ 0.2	2.3 $\pm$ 0.2
TRIG (mg/dL)	201.2 $\pm$ 43.8	178.2 $\pm$ 65.3	156.0 $\pm$ 28.5

<sup>a</sup>Biochemical parameters includes cholesterol (CHOL), creatine kinase (CK), alanine aminotransferase (ALT), aspartate aminotransferase (AST), alkaline phosphatase (ALP), total bilirubin (TBILI), total protein (TPROT), glucose (GLU), inorganic phosphorus (PHOS), calcium (CA), carbon dioxide (CO<sub>2</sub>\_LC), blood urea nitrogen (BUN), creatinine (CREAT), direct bilirubin (DBILI), albumin (ALB), albumin-globulin ratio (AGR), blood creatinine (B-CREA), amylase (AMYL), lactate dehydrogenase (LDH), magnesium (Mg), triglycerides (TRIG). There is no statistical significance between each group as analyzed by one-way ANOVA.

branes, it would be clearly necessary to conduct studies to demonstrate the therapeutic efficiency of the MSNP platform *in vivo*. To date, only limited *in vivo* data have been published regarding the toxicity, biodistribution, and biopersistence of MSNP.<sup>1,48–50</sup> Coating of MSNP by MRI agents has been used to perform *in vivo* imaging; this demonstrated that the particles could still be detected in the circulation 30 min after administration, but then

## MATERIALS AND METHODS

**Reagents.** Tetraethylorthosilicate (98%), cetyltrimethylammonium bromide (CTAB, 95%), fluorescein isothiocyanate (FITC, 90%), polyethyleneimine (MW 1.2 and 25 kD), poly(ethylene glycol) methyl ether (MW 5 kD), *N,N'*-disuccinimidyl carbonate (DSC, 95%), 4-(dimethylamino)pyridine (DMAP, 99%), aminopropyltriethoxysilane (APTS, 99%), 3-(trihydroxysilyl)propyl methylphosphonate (42%), succinic anhydride (99%), fluorescamine, paclitaxel, propidium iodide (PI),  $\beta$ -actin antibody, and bovine serum albumin (BSA) were from Sigma (St. Louis, MO). Polyethyleneimine (MW 0.6, 1.8, and 10 kD) were from Alfa Aesar (Ward Hill, MA). The MTS assay kit was from Promega (Madison, WI). Dulbecco's Modified Eagle's medium (DMEM), penicillin/streptomycin, and L-glutamine were purchased from Invitrogen (Carlsbad, CA). Fetal calf serum (FCS) was from Atlanta Biologicals, Inc. (Lawrenceville, GA). siRNA for GFP knockdown was purchased from IDT Technologies (Coralville, IA). For all experiments and analyses, water was deionized and filtered with a 0.45  $\mu$ m pore size polycarbonate syringe filter (Millipore, Billerica, MA). All

accumulate in the RES system such as liver and spleen, with less signal coming from the kidney, lung, and heart.<sup>1,50</sup> Another interesting finding is that MSNP accumulate preferentially at tumor sites through an enhanced permeability and retention (EPR) effect.<sup>1</sup> To achieve the full potential of MSNP, detailed *in vivo* testing should be done to assess biodistribution, pharmacokinetics, and targeting. It is encouraging that our *in vivo* safety study did not show any signs of toxicity after intravenous injection, including for particles coated by the 25 kD polymer. The lack of *in vivo* toxicity in spite of the *in vitro* cytotoxic effects can best be explained by the dilution of the particles in the circulatory system and the strong defense capabilities of the body against foreign substances. The extent to which these protective mechanisms may interfere with the effectiveness of drug delivery still needs to be determined but could be dealt with in a rational fashion by dynamic design features such as demonstrated in this study.

## CONCLUSION

Polyethyleneimine-coated mesoporous silica nanoparticle is a versatile delivery system that can facilitate cellular uptake to increase drug delivery payload and also be utilized to improve nucleic acids delivery for therapeutic and experimental use. While the potential cytotoxicity of PEI attachment could interfere with the efficacy of siRNA delivery, it is possible by selecting optimal polymer lengths to maintain high transfection efficiency while simultaneously reducing or eliminating toxic effects. While inefficient for gene delivery, coating with low molecular weight PEI polymers is nonetheless efficient to increase delivery of antitumor drug paclitaxel into cancer cells. These hybrid organic–inorganic porous nanoparticles can potentially be useful for the simultaneous delivery of nucleotides and small molecules into cells.

chemicals were reagent grade and used without further purification or modification.

**Synthesis and Surface Modification of Mesoporous Silica Nanoparticles MSNP.** The basic synthesis of MSNP was conducted by mixing the silicate source tetraethylorthosilicate (TEOS) with the templating surfactants cetyltrimethylammonium bromide (CTAB) in basic aqueous solution (pH 11). In a round-bottom flask, 100 mg of CTAB was dissolved in a solution of 48 mL of distilled water and 0.35 mL of sodium hydroxide (2 M). The solution was heated to 80 °C and stirred vigorously. After the temperature had stabilized, 0.5 mL of TEOS was added slowly into the heated CTAB solution. After 15 min, 0.23 mmol of the organosilane solution was added into the mixture. 3-Trihydroxysilylpropyl methylphosphonate was used for phosphonate surface modification, and aminopropyltriethoxy silane (APTS) was used for amine surface modification. After 2 h, the solution was cooled to room temperature, and the materials were washed with methanol using centrifugation. In order to incorporate fluorescent dye molecules in the silicate framework, fluorescein-modified silane was first synthesized and then mixed with TEOS. To synthesize fluorescein-

modified silane, 2.4  $\mu\text{L}$  of APTS was mixed with 1 mg of fluorescein isothiocyanate (FITC) in 0.6 mL of absolute ethanol and stirred for 2 h under inert atmosphere. In another formulation, rhodamine-B isothiocyanate (RITC) was used instead of FITC to synthesize rhodamine-B-modified APTS. The dye-modified silane was then mixed with TEOS before adding the mixture into the heated CTAB solution. The surfactants were removed from the pores by refluxing the particles in a mixture of 20 mL of methanol and 1 mL of hydrochloric acid (12.1 M) for 24 h. The materials were then centrifuged and washed with methanol.

For the poly(ethylene glycol) modification, 1 g of poly(ethylene glycol) methyl ether (MW 5 kD, mPEG) was dried under vacuum for 30 min and dissolved in 5 mL of dioxane (with slight heating). mPEG has only one reactive end that can be attached to the particle surface and limits the coupling process only to that end, whereas normal PEG has two reactive ends and may cause particle cross-linking; 307.4 mg of disuccinimidyl carbonate (DSC) was dissolved in 2 mL of anhydrous DMF (with slight heating) and mixed with the mPEG solution; 146.6 mg of 4-(dimethylamino)pyridine was dissolved in 2 mL of acetone and added slowly into the mPEG solution. The mixture was stirred for 6 h under an inert atmosphere. The polymer was precipitated by the addition of 30 mL of diethyl ether to the solution and separated by centrifugation. After washing the polymer twice with diethyl ether, the activated mPEG was dried under vacuum. Sixty milligrams of amine-modified MSNP was washed and resuspended in 2 mL of anhydrous DMF; 300 mg of the activated mPEG was dissolved in 9 mL of DMF and mixed with the particles. The mixture was stirred for 12 h and washed thoroughly with DMF and PBS.

To perform polyethyleneimine (PEI) modification, 5 mg of phosphonate-modified MSNP was dispersed in a solution of 2.5 mg of PEI (MW 25 kD) and 1 mL of absolute ethanol. The process to coat the particles with other PEI polymers (MW 0.6, 1.2, 1.8, 10 kD) was carried out similarly. After the mixture was sonicated and stirred for 30 min, the particles coated with PEI were washed with ethanol and PBS. Thermogravimetric analysis showed that the amount of PEI on the particles was approximately 5 wt %. To succinylate the PEI 25 kD-coated particles, 1 mg particles was resuspended in 0.25 mL of anhydrous DMF and mixed with different amounts of succinic anhydride (0.15, 0.075, and 0.015 mg). The mixture was sonicated and stirred overnight. The succinylated particles were washed with DMF and resuspended in PBS. To fluorescently label PEI (MW 25 kD), 60 mg of PEI 25 kD was dissolved in 10 mL of carbonate buffer (pH 9) and mixed with 1 mg of rhodamine-B isothiocyanate dissolved in 1 mL of DMSO. The mixture was stirred for 24 h at 4 °C and dialyzed against distilled water. The rhodamine-B-labeled PEI 25 kD was attached to the particles by using similar procedure for the unlabeled PEI.

**Physicochemical Characterization.** All MSNP were characterized for size, size distribution, shape, and charge (Table 1). The shape and structure were characterized using a transmission electron microscope (JEOL JEM 2010, JEOL USA, Inc., Peabody, MA). Microfilms for TEM imaging were made by placing a drop of the respective particle suspension onto a 200-mesh copper TEM grid (Electron Microscopy Sciences, Washington, PA) and then drying at room temperature overnight. A minimum of five images of each sample was collected to obtain representative views. Particle size and  $\zeta$  potential in solution were measured by ZetaSizer Nano (Malvern Instruments Ltd., Worcestershire, UK). This instrument measures the light scattering (DLS) from a suspension at an angle of 173°. Size measurements were performed on dilute suspensions in water or complete cell culture media at pH 7.4. The ZetaSizer Nano was also used to measure the electrophoretic mobility of the MSNP suspended in solution. Electrophoretic mobility is used as an approximation of particle surface charge and can be used to calculate  $\zeta$  potential. The Helmholtz–Smolouchowski equation was used to recalculate electrophoretic mobility into  $\zeta$  potential.

**Drug Loading of Paclitaxel.** The modified materials were loaded with paclitaxel by incubating 10 mg of the nanoparticles in a solution of 1 mg of paclitaxel and 0.25 mL of DMSO for 6 h. After the drug-laden nanoparticles were removed from the suspension by centrifugation and the supernatant was removed com-

pletely, the materials were dried under vacuum. The drug-laden nanoparticles were washed and sonicated with PBS. In order to determine the amount of paclitaxel that partitioned to the MSNP, the aqueous particle suspension was incubated for 6 h at 4 °C before centrifugation. Methanol was used to release paclitaxel from MSNP to determine the loading capacity. The drug-laden MSNP pellet was resuspended and sonicated in methanol on three occasions, and the supernatants were combined to measure the release of the drug by UV absorption at 230 nm; 50  $\mu\text{g}/\text{mL}$  particles contained about 1  $\mu\text{M}$  of paclitaxel.

**MSNP Dispersion and Use To Perform Tissue Culture.** All cell cultures were maintained in 25  $\text{cm}^2$  cell culture flasks in which the cells were passaged at 70–80% confluency every 2–4 days. RAW 264.7, BxPC3, PANC-1, and HEPA-1 cell lines were cultured in Dulbecco's Modified Eagle Medium (DMEM) (Carlsbad, CA) containing 10% fetal calf serum (FCS), 100 U/mL penicillin, 100  $\mu\text{g}/\text{mL}$  streptomycin, and 2 mM L-glutamine (complete medium). BEAS-2B cells were cultured in BEGM (Charles City, IA) in type I rat tail collagen-coated flasks or plates. Cells were cultured at 37 °C in a humidified 5%  $\text{CO}_2$  atmosphere. To disperse MSNP, the stock solution (in water) was sonicated (Tekmar Sonic Disruptor probe) for 15 s prior to aliquoting. In order to coat the surface of MSNP with bovine serum albumin (BSA), the aliquoted NP suspension ( $\sim 10 \mu\text{L}$ ) was mixed with an equal volume of 4% BSA. Tissue culture media (1 mL) was added to the BSA-coated MSNP suspension. Cell culture media deprived of serum (e.g., BEGM) was modified by addition of BSA at a concentration of 2  $\text{mg}/\text{mL}$ . The cell culture media containing MSNP at the desired concentration was sonicated for 15 s and characterized as described before.

**Assays for Cellular Viability and Mitochondrial Function.** Cellular viability was determined by the MTS assay, which looks at the reduction of (3-(4,5-dimethylthiazol-2-yl)-5-(3-carboxymethoxyphenyl)-2-(4-sulfophenyl)-2H-tetrazolium (MTS) to formazan in viable cells. Briefly,  $2 \times 10^4$  cells were plated onto 96-multi-well plates (Costar; Corning, NY). After incubation with the indicated dose of MSNP for various lengths of time at 37 °C, formazan absorbance was measured at 490 nm. The mean absorbance of nonexposed cells served as the reference for calculating 100% cellular viability.

Cell death and mitochondrial function were detected using propidium iodide (PI) uptake and JC-1 fluorescence. Fluorescent probes were diluted in DMEM before the addition to cells for 30 min at 37 °C in the dark: (i) 5  $\mu\text{g}/\text{mL}$  propidium iodide (PI) in 200  $\mu\text{L}$  of DMEM (assessment of cell death); (ii) 5  $\mu\text{M}$  JC-1 (assessment of  $\Delta\Psi\text{m}$ ). Flow cytometry was performed using a LSR (Becton Dickinson, Mountain View, CA). PI was analyzed in FL-2, and JC-1 was analyzed in both FL-1 and FL-2. Forward and side scatter were used to gate out cellular fragments.

**Assessment of Cellular MSNP Uptake by Flow Cytometry and Confocal Microscopy.** For the performance of flow cytometry, aliquots of  $5 \times 10^4$  cells (RAW 264.7, BEAS-2B, PANC-1, and BxPC3) were cultured in 48-well plates in 0.4 mL of medium. RITC-labeled MSNP with a phosphonate surface coating were added to the above cultures at a dose of 25  $\mu\text{g}/\text{mL}$  for 30 min, followed by incubation with the FITC-labeled MSNP-PEI series at final concentrations of 25  $\mu\text{g}/\text{mL}$  for 3 h. All cell types were trypsinized and washed with trypan blue to quench the fluorescence of cell-surface-attached MSNP. Cells were analyzed in a LSR flow cytometer using mean FL-2 and FL-1 to assess RITC and FITC fluorescence, respectively. Data are reported as fold increase above control (cells without MSNP).

Cellular uptake of MSNP was performed by adding 25  $\mu\text{g}/\text{mL}$  of the various MSNP to 8-well chamber slides (Nunc) in which  $5 \times 10^4$  cells were cultured in each well containing 0.4 mL culture medium. Cell membranes were stained with 5  $\mu\text{g}/\text{mL}$  wheat germ agglutinin (WGA) Alexa Fluor 594 conjugate in PBS for 30 min. Slides were mounted with DAPI (Molecular Probes, Eugene, OR) and visualized under a confocal microscope (Leica Confocal 1P/FCS) in the UCLA/CNSI Advanced Light Microscopy/Spectroscopy Shared Facility. High-magnification images were obtained with a 63 $\times$  objective. Optical sections were averaged 2–4 times to reduce noise. Images were processed using Leica Confocal Software.



**Preparation of PEI-MSNPs—pDNA/siRNA Polyplexes and Agarose Gel Retardation.** Agarose gel retardation assay was used to determine the DNA/siRNA binding ability of PEI-coated MSNP; 0.1  $\mu\text{g}$  of plasmid DNA (pEGFP) or siRNA in aqueous solution was used to mix with PEI-coated nanoparticles to obtain particle to pDNA ratios (N/P) ratios of 5–600. The mixture was incubated at room temperature for 30 min for complex formation. Ten microliters of the polyplex solution mixed with 2  $\mu\text{L}$  of  $6\times$  loading buffer was electrophoresed on 1% agarose gel containing 0.5  $\mu\text{g}/\text{mL}$  ethidium bromide (EB) with Tris-boric acid (TBE) running buffer (pH 8) at 100 V for 30 min. DNA/RNA bands were visualized by UV (254 nm) illuminator and photographed with a Bio-Rad imaging system (Hercules, CA). The binding capacity was expressed by the N/P ratio that shows total retardation of DNA or siRNA migration (as reflected by the disappearance of DNA/RNA bands on the gel).

**DNase I Protection Assay:** Particle/pDNA complexes were prepared at a MSNP/pDNA ratio of 100 with 100 ng of pDNA in 10  $\mu\text{L}$  total volume. The complex solutions were incubated with 1  $\mu\text{L}$  of DNase I (2.7 U/ $\mu\text{L}$ ) in 50 mM Tris-Cl, 10 mM  $\text{MgCl}_2$ , pH 7.4, at 37  $^\circ\text{C}$  for 30 min. The DNase I was inactivated by adding 1  $\mu\text{L}$  of 100 mM ethylenediaminetetraacetic acid (EDTA). The pDNA was then released from the complex by adding 1% sodium dodecyl sulfate (SDS) and analyzed by 1% agarose gel electrophoresis.

**Plasmid DNA and siRNA Transfection with the Use of MSNP-PEI.** Plasmid DNA (pDNA) containing a GFP insert was used to transfect HEPA-1 cells cultured either in Nunc chamber slides for performance of confocal microscopy or in 48-well plates for assessment by flow cytometry. Cells were plated at a density of  $2 \times 10^4$  cells per well in 0.4 mL of medium. pDNA/MSNP complexes were prepared by mixing 100 ng/mL of DNA with 25  $\mu\text{g}/\text{mL}$  of MSNP for 30 min prior to cellular incubation for 24 h. Cells were fixed for confocal microscopy as described above. Harvested cells were used to conduct flow cytometry on FL-1 channel.

To perform siRNA experiments, HEPA-1 cells were prior transfected with a GFP plasmid and then sorted in the FL-1 channel to select stable GFP expressing cells. The sorted cells were plated at a density of  $5 \times 10^4$  cells per well containing 0.4 mL culture medium in chamber slides for performance of confocal microscopy and in 48-well plates for performance of flow cytometry. MSNP/siRNA complexes were prepared by incubating 500 ng/mL of siRNA with 25  $\mu\text{g}/\text{mL}$  of MSNP-PEI for 30 min in serum-free DMEM. Cells were then exposed to the complexes for 3 h. DMEM + 10% FCS was then added to bring the final volume to 400  $\mu\text{L}$  for 48 h. Cells were fixed and prepared for confocal microscopy as described above. For flow cytometry, cells were harvested and analyzed for fold decrease in GFP expression (FL-1 channel).

**Paclitaxel Delivery by MSNP-PEI.** PANC-1 and BxPC3 cells were plated at  $2 \times 10^4$  cells per well in a 96-well plate. MSNP particles, loaded with paclitaxel, were incubated with the cells at doses of 10–50  $\mu\text{g}/\text{mL}$  for 48–72 h. Free paclitaxel corresponding to the amount loaded into MSNP particles was suspended or dissolved in PBS and DMSO to serve as controls. MTS assays were performed after 48 h to determine the cell viability after treatment.

**In Vivo MSNP Toxicity Testing.** Animal experiment protocols were reviewed and approved by the Chancellor's Animal Research Committee (ARC) at UCLA. Animal experiments were performed in accordance with UCLA guidelines for care and treatment of laboratory animals and the NIH Guide for the Care and Use of Laboratory Animals in Research (DHEW78-23). The mice were randomly divided into three groups: MSNP-phosphonate, MSNP-PEI 25 kD, and the saline control group. We used six mice per group since this number has enough statistical power to discern differences in the toxic responses. We used 40 mg/kg particles for intravenous injection through tail vein once a week for 2 weeks. Animal weight was monitored after particle injections. Animals were sacrificed later to obtain blood and organs.

**Biochemical Serum Assays.** The serum was obtained by centrifuging the whole blood at 3000 rpm for 15 min. The biochemical parameters were assayed by UCLA Division of Laboratory Animal Medicine (DLAM) diagnostic laboratory services.

**Histology of Major Organs.** A small piece of liver, kidney, spleen, lung, heart, and brain was fixed by 10% formalin and then em-

bedded into paraffin, sectioned for 5  $\mu\text{m}$  thick, and mounted on the glass microscope slides by UCLA Division of Laboratory Animal Medicine (DLAM) diagnostic laboratory services. The sections were stained with hematoxylin-eosin and examined by light microscopy. The slides were read by an experienced veterinary pathologist.

**Statistical Analysis.** All data are expressed as the mean  $\pm$  standard deviation. An unpaired Student's *t* test was used to assess the difference between two groups. One-way ANOVA was performed when more than two groups were compared with a single control. Differences between individual groups within the set were assessed by a multiple comparison test (Tukey) when the *F* statistic was  $<0.05$ . A  $p < 0.05$  was considered significant.

**Acknowledgment.** This work is supported by the National Science Foundation and the Environmental Protection Agency under Cooperative Agreement Number EF 0830117. Any opinions, findings, conclusions, or recommendations expressed herein are those of the author(s) and do not necessarily reflect the views of the National Science Foundation or the Environmental Protection Agency. This work has not been subjected to an EPA peer and policy review. Key support was provided by the UC Lead Campus for Nanotoxicology Training and Research, funded by UC TSR&TP, US Public Health Service Grants (U19 AI070453, R01 ES016746, and R01 ES015498) and the US EPA STAR award (RD-83241301) to the Southern California Particle Center. Key support was also provided by the grant USDOD HDTRA 1-08-1-0041. Fluorescent microscopy was performed at the CNSI Advanced Light Microscopy/Spectroscopy Shared Facility at UCLA.

**Note added after ASAP publication:** In the version published ASAP September 9, 2009, Figure 5 was missing the  $\Phi$  labels, and Figure 8 was missing  $\mu$  prefixes in the axis labels. The corrected version was published ASAP September 18, 2009.

**Supporting Information Available:** Particle size distribution, cell viability, surface modification and fluorescent labeling of PEI-MSNPs, flow cytometry, and confocal microscopy for cellular uptake. This material is available free of charge via the Internet at <http://pubs.acs.org>.

## REFERENCES AND NOTES

- Kim, J.; Kim, H. S.; Lee, N.; Kim, T.; Kim, H.; Yu, T.; Song, I. C.; Moon, W. K.; Hyeon, T. Multifunctional Uniform Nanoparticles Composed of a Magnetite Nanocrystal Core and a Mesoporous Silica Shell for Magnetic Resonance and Fluorescence Imaging and for Drug Delivery. *Angew. Chem., Int. Ed.* **2008**, *47*, 8438–8441.
- Liong, M.; Lu, J.; Kovichich, M.; Xia, T.; Ruehm, S. G.; Nel, A. E.; Tamanoi, F.; Zink, J. I. Multifunctional Inorganic Nanoparticles for Imaging, Targeting, and Drug Delivery. *ACS Nano* **2008**, *2*, 889–896.
- Lu, J.; Liong, M.; Zink, J. I.; Tamanoi, F. Mesoporous Silica Nanoparticles as a Delivery System for Hydrophobic Anticancer Drugs. *Small* **2007**, *3*, 1341–1346.
- Slowing, I. I.; Vivero-Escoto, J. L.; Wu, C.-W.; Lin, V. S.-Y. Mesoporous Silica Nanoparticles as Controlled Release Drug Delivery and Gene Transfection Carriers. *Adv. Drug Delivery Rev.* **2008**, *60*, 1278–1288.
- Vallet-Regi, M.; Balas, F.; Arcos, D. Mesoporous Materials for Drug Delivery. *Angew. Chem., Int. Ed.* **2007**, *46*, 7548–7558.
- Borm, P.; Klaessig, F. C.; Landry, T. D.; Moudgil, B.; Pauluhn, J.; Thomas, K.; Trotter, R.; Wood, S. Research Strategies for Safety Evaluation of Nanomaterials, Part V: Role of Dissolution in Biological Fate and Effects of Nanoscale Particles. *Toxicol. Sci.* **2006**, *90*, 23–32.
- Finnie, K.; Waller, D.; Perret, F.; Krause-Heuer, A.; Lin, H.; Hanna, J.; Barbé, C. Biodegradability of Sol–Gel Silica Microparticles for Drug Delivery. *J. Sol–Gel Technol.* **2009**, *49*, 12–18.

8. Vivero-Escoto, J. L.; Slowing, I. I.; Wu, C.-W.; Lin, V. S.-Y. Photoinduced Intracellular Controlled Release Drug Delivery in Human Cells by Gold-Capped Mesoporous Silica Nanosphere. *J. Am. Chem. Soc.* **2009**, *131*, 3462–3463.
9. Nguyen, T. D.; Leung, K. C. F.; Liong, M.; Pentecost, C. D.; Stoddart, J. F.; Zink, J. I. Construction of a pH-Driven Supramolecular Nanovalve. *Org. Lett.* **2006**, *8*, 3363–3366.
10. Rosenholm, J. M.; Meinander, A.; Peuhu, E.; Niemi, R.; Eriksson, J. E.; Sahlgren, C.; Linde, M. Targeting of Porous Hybrid Silica Nanoparticles to Cancer Cells. *ACS Nano* **2009**, *3*, 197–206.
11. Park, I. Y.; Kim, I. Y.; Yoo, M. K.; Choi, Y. J.; Cho, M.-H.; Cho, C. S. Mannosylated Polyethyleneimine Coupled Mesoporous Silica Nanoparticles for Receptor-Mediated Gene Delivery. *Int. J. Pharm.* **2008**, *359*, 280–287.
12. Radu, D. R.; Lai, C. Y.; Jęftiniija, K.; Rowe, E. W.; Jęftiniija, S.; Lin, V. S. Y. A Polyamidoamine Dendrimer-Capped Mesoporous Silica Nanosphere-Based Gene Transfection Reagent. *J. Am. Chem. Soc.* **2004**, *126*, 13216–13217.
13. Torney, F.; Trewyn, B. G.; Lin, V. S.-Y.; Wang, K. Mesoporous Silica Nanoparticles Deliver DNA and Chemicals into Plants. *Nat. Nanotechnol.* **2007**, *2*, 295–300.
14. Bharali, D. J.; Klejbor, I.; Stachowiak, E. K.; Dutta, P.; Roy, I.; Kaur, N.; Bergey, E. J.; Prasad, P. N.; Stachowiak, M. K. Organically Modified Silica Nanoparticles: A Nonviral Vector for *In Vivo* Gene Delivery and Expression in the Brain. *Proc. Natl. Acad. Sci. U.S.A.* **2005**, *102*, 11539–11544.
15. Bonoiu, A. C.; Mahajan, S. D.; Ding, H.; Roy, I.; Yong, K.-T.; Kumar, R.; Hu, R.; Bergey, E. J.; Schwartz, S. A.; Prasad, P. N. Nanotechnology Approach for Drug Addiction Therapy: Gene Silencing Using Delivery of Gold Nanorod–siRNA Nanoplex in Dopaminergic Neurons. *Proc. Natl. Acad. Sci. U.S.A.* **2009**, *106*, 5546–5550.
16. Elbakry, A.; Zaky, A.; Liebl, R.; Rachel, R.; Goepferich, A.; Breuning, M. Layer-by-Layer Assembled Gold Nanoparticles for siRNA Delivery. *Nano Lett.* **2009**, *9*, 2059–2064.
17. Fuller, J. E.; Zugates, G. T.; Ferreira, L. S.; Ow, H. S.; Nguyen, N. N.; Wiesner, U. B.; Langer, R. S. Intracellular Delivery of Core–Shell Fluorescent Silica Nanoparticles. *Biomaterials* **2008**, *29*, 1526–1532.
18. Kneuer, C.; Sameti, M.; Bakowsky, U.; Schiestel, T.; Schirra, H.; Schmidt, H.; Lehr, C.-M. A Nonviral DNA Delivery System Based on Surface Modified Silica-Nanoparticles Can Efficiently Transfect Cells *In Vitro*. *Bioconjugate Chem.* **2000**, *11*, 926–932.
19. McBain, S. C.; Yiu, H. H. P.; Haj, A. E.; Dobson, J. Polyethyleneimine Functionalized Iron Oxide Nanoparticles as Agents for DNA Delivery and Transfection. *J. Mater. Chem.* **2007**, *17*, 2561–2565.
20. Zhu, S.-G.; Xiang, J.-J.; Li, X.-L.; Shen, S.-R.; Lu, H.-b.; Zhou, J.; Xiong, W.; Zhang, B.-C.; Nie, X.-M.; Zhou, M.; Tang, K. Gui-Yuan, Poly(L-lysine)-Modified Silica Nanoparticles for the Delivery of Antisense Oligonucleotides. *Biotechnol. Appl. Biochem.* **2004**, *39*, 179–187.
21. Boussif, O.; Lezoualc'h, F.; Zanta, M. A.; Mergny, M. D.; Scherman, D.; Demeneix, B.; Behr, J. P. A Versatile Vector for Gene and Oligonucleotide Transfer into Cells in Culture and *In Vivo*: Polyethyleneimine. *Proc. Natl. Acad. Sci. U.S.A.* **1995**, *92*, 7297–7301.
22. Godbey, W. T.; Wu, K. K.; Mikos, A. G. Tracking the Intracellular Path of Poly(ethyleneimine)/DNA Complexes for Gene Delivery. *Proc. Natl. Acad. Sci. U.S.A.* **1999**, *96*, 5177–5181.
23. Urban-Klein, B.; Werth, S.; Abuharbeid, S.; Czubayko, F.; Aigner, A. RNAi-Mediated Gene-Targeting through Systemic Application of Polyethyleneimine (PEI)-Complexed siRNA *In Vivo*. *Gene Ther.* **2005**, *12*, 461–466.
24. Liong, M.; France, B.; Bradley, K. A.; Zink, J. I. Antimicrobial Activity of Silver Nanocrystals Encapsulated in Mesoporous Silica Nanoparticles. *Adv. Mater.* **2009**, *21*, 1684–1689.
25. Duan, H.; Nie, S. Cell-Penetrating Quantum Dots Based on Multivalent and Endosome-Disrupting Surface Coatings. *J. Am. Chem. Soc.* **2006**, *129*, 3333–3338.
26. Florea, B. I.; Meaney, C.; Junginger, H. E.; Borchard, G. Transfection Efficiency and Toxicity of Polyethyleneimine in Differentiated Calu-3 and Nondifferentiated COS-1 Cell Cultures. *AAPS PharmSci.* **2002**, *4*, E12.
27. Neu, M.; Fischer, D.; Kissel, T. Recent Advances in Rational Gene Transfer Vector Design Based on Poly(ethyleneimine) and Its Derivatives. *J. Gene. Med.* **2005**, *7*, 992–1009.
28. Xia, T.; Kovochich, M.; Brant, J.; Hotze, M.; Sempf, J.; Oberley, T.; Sioutas, C.; Yeh, J. I.; Wiesner, M. R.; Nel, A. E. Comparison of the Abilities of Ambient and Manufactured Nanoparticles to Induce Cellular Toxicity According to An Oxidative Stress Paradigm. *Nano Lett.* **2006**, *6*, 1794–1807.
29. Xia, T.; Kovochich, M.; Liong, M.; Zink, J. I.; Nel, A. E. Cationic Polystyrene Nanosphere Toxicity Depends on Cell-Specific Endocytic and Mitochondrial Injury Pathways. *ACS Nano* **2008**, *2*, 85–96.
30. Cai, Q.; Luo, Z.-S.; Pang, W.-Q.; Fan, Y.-W.; Chen, X.-H.; Cui, F.-Z. Dilute Solution Routes to Various Controllable Morphologies of MCM-41 Silica with a Basic Medium. *Chem. Mater.* **2001**, *13*, 258–263.
31. Xia, T.; Kovochich, M.; Liong, M.; Madler, L.; Gilbert, B.; Shi, H.; Yeh, J. I.; Zink, J. I.; Nel, A. E. Comparison of the Mechanism of Toxicity of Zinc Oxide and Cerium Oxide Nanoparticles Based on Dissolution and Oxidative Stress Properties. *ACS Nano* **2008**, *2*, 2121–2134.
32. Moazed, D. Small RNAs in Transcriptional Gene Silencing and Genome Defence. *Nature* **2009**, *457*, 413–420.
33. Blow, N. Small RNAs: Delivering the Future. *Nature* **2007**, *450*, 1117–1120.
34. Davis, M. E. The First Targeted Delivery of siRNA in Humans *via* a Self-Assembling, Cyclodextrin Polymer-Based Nanoparticle: From Concept to Clinic. *Mol. Pharm.* **2009**, *6*, 659–668.
35. Judge, A. D.; Bola, G.; Lee, A. C. H.; MacLachlan, I. Design of Noninflammatory Synthetic siRNA Mediating Potent Gene Silencing *In Vivo*. *Mol. Ther.* **2006**, *13*, 494–505.
36. Ludwig, J. A.; Szakacs, G.; Martin, S. E.; Chu, B. F.; Cardarelli, C.; Sauna, Z. E.; Caplen, N. J.; Fales, H. M.; Ambudkar, S. V.; Weinstein, J. N.; Gottesman, M. M. Selective Toxicity of NSC73306 in MDR1-Positive Cells as a New Strategy to Circumvent Multidrug Resistance in Cancer. *Cancer Res.* **2006**, *66*, 4808–4815.
37. Kircheis, R.; Schuller, S.; Brunner, S.; Ogris, M.; Heider, K. H.; Zauner, W.; Wagner, E. Polycation-Based DNA Complexes for Tumor-Targeted Gene Delivery *In Vivo*. *J. Gene. Med.* **1999**, *1*, 111–120.
38. Yezhelyev, M. V.; Qi, L.; O'Regan, R. M.; Nie, S.; Gao, X. Proton-Sponge Coated Quantum Dots for siRNA Delivery and Intracellular Imaging. *J. Am. Chem. Soc.* **2008**, *130*, 9006–9012.
39. Sonawane, N. D.; Thiagarajah, J. R.; Verkman, A. S. Chloride Concentration in Endosomes Measured Using a Ratioable Fluorescent Cl<sup>-</sup> Indicator: Evidence for Chloride Accumulation During Acidification. *J. Biol. Chem.* **2002**, *277*, 5506–5513.
40. Clottens, F. L.; Verbeken, E. K.; Demedts, M.; Nemery, B. Pulmonary Toxicity of Components of Textile Paint Linked to the Ardystil Syndrome: Intratracheal Administration in Hamsters. *Occup. Environ. Med.* **1997**, *54*, 376–387.
41. Hoet, P. H.; Gilissen, L.; Nemery, B. Polyanions Protect Against the *In Vitro* Pulmonary Toxicity of Polycationic Paint Components Associated with the Ardystil Syndrome. *Toxicol. Appl. Pharmacol.* **2001**, *175*, 184–190.
42. Hoet, P. H.; Gilissen, L. P.; Leyva, M.; Nemery, B. *In vitro* Cytotoxicity of Textile Paint Components Linked to the “Ardystil Syndrome”. *Toxicol. Sci.* **1999**, *52*, 209–216.
43. Nel, A. E.; Madler, L.; Velegol, D.; Xia, T.; Hoek, E. M.; Somasundaran, P.; Klaessig, F.; Castranova, V.; Thompson, M. Understanding Biophysicochemical Interactions at the Nano-Bio Interface. *Nat. Mater.* **2009**, *8*, 543–557.
44. Shim, M. S.; Kwon, Y. J. Controlled Cytoplasmic and Nuclear Localization of Plasmid DNA and siRNA by Differentially Tailored Polyethyleneimine. *J. Controlled Release* **2009**, *133*, 206–213.

45. Veisoh, O.; Kievit, F. M.; Gunn, J. W.; Ratner, B. D.; Zhang, M. A Ligand-Mediated Nanovector for Targeted Gene Delivery and Transfection in Cancer Cells. *Biomaterials* **2009**, *30*, 649–657.
46. Hobel, S.; Prinz, R.; Malek, A.; Urban-Klein, B.; Sitterberg, J.; Bakowsky, U.; Czubayko, F.; Aigner, A. Polyethylenimine PEI F25-LMW Allows the Long-Term Storage of Frozen Complexes as Fully Active Reagents in siRNA-Mediated Gene Targeting and DNA Delivery. *Eur. J. Pharm. Biopharm.* **2008**, *70*, 29–41.
47. Peng, Q.; Hu, C.; Cheng, J.; Zhong, Z.; Zhuo, R. Influence of Disulfide Density and Molecular Weight on Disulfide Cross-Linked Polyethylenimine as Gene Vectors. *Bioconjugate Chem.* **2009**, *20*, 340–346.
48. Barb, C.; Bartlett, J.; Kong, L.; Finnie, K.; Lin, H.; Larkin, M.; Calleja, S.; Bush, A.; Calleja, G. Silica Particles: A Novel Drug-Delivery System. *Adv. Mater.* **2004**, *16*, 1959–1966.
49. Taylor, K. M. L.; Kim, J. S.; Rieter, W. J.; An, H.; Lin, W.; Lin, W. Mesoporous Silica Nanospheres as Highly Efficient MRI Contrast Agents. *J. Am. Chem. Soc.* **2008**, *130*, 2154–2155.
50. Wu, S.-H.; Lin, Y.-S.; Hung, Y.; Chou, Y.-H.; Hsu, Y.-H.; Chang, C.; Mou, C.-Y. Multifunctional Mesoporous Silica Nanoparticles for Intracellular Labeling and Animal Magnetic Resonance Imaging Studies. *ChemBioChem* **2008**, *9*, 53–57.